

Magnetic ripple domain structure in FeGa/MgO thin films

Adrián Begué,^{1,2} Maria Grazia Proietti,^{1,2} José I. Arnaudas,^{1,2,3} and Miguel Ciria^{1,2,*}

¹*Instituto de Ciencia de Materiales de Aragón, Consejo Superior de Investigaciones Científicas, Zaragoza, Spain.*

²*Departamento de Física de la Materia Condensada, Universidad de Zaragoza, Zaragoza, Spain.*

³*Instituto de Nanociencia de Aragón, Universidad de Zaragoza, Zaragoza, Spain.*

(Dated: May 23, 2019)

The magnetic domain structure is studied in epitaxial Fe_{100-x}Ga_x/MgO(001) films with $0 < x < 30$ and thicknesses below 60 nm by magnetic force microscopy. For low gallium content, domains with the magnetization lying in the film plane and domain walls separating micrometric areas are observed. Above $x \approx 20$, the magnetic contrast shows a fine corrugation, ranging from 300 to 900 nm, suggesting a ripple substructure with a periodic oscillation of the magnetization. We discuss the presence of a random magnetic anisotropy contribution, that superimposed to the cubic coherent anisotropy, is able to break the uniform orientation of the magnetization. The origin of that random anisotropy is attributed to several factors: coexistence of crystal phases in the films, inhomogeneous distribution of both internal strain and Ga-Ga next nearest neighbor pairs and interface magnetic anisotropy due to the Fe-O bond.

INTRODUCTION

The Fe-Ga alloys have become an important material for magnetostrictive applications because of their large tetragonal magnetostriction λ_{100} at low field [1–3] enhanced by the presence of rare earth impurities [4]. Bulk samples preparation includes or combines slow cooling, quenching and annealing and can provide a number of microstructures depending on procedure and composition, thus the D0₃ high temperature phase can be obtained instead of a mix of A2 disorder *bcc* and ordered L1₂ *fcc* crystal phases [5]. The magnetic properties look to be controlled by the presence of next-nearest neighbors (NNN) Ga-Ga pairs along the cubic [100] directions and its relation with the magnetostrictive is suggested by the presence of heterogeneous inclusions with tetragonal distortion [4]. These micro- or nano-domains regions are defined by a correlation in the distribution of Ga-Ga pairing, and the rotation of the magnetization M of the cubic A2 matrix in the presence of these inclusions is addressed as the responsible of the large magnetostriction in the FeGa alloys [4]. The Ga pairing along the [100] direction has been also linked to the decrement of the cubic magnetocrystalline four-fold anisotropy constant in this compound [6]. The magnetic behavior is enriched in thin films systems, and a perpendicular magnetic anisotropy (PMA) in epitaxial films is ascribed to a minute asymmetric distribution of these NNN Ga-Ga pairs between the film in-plane and out-of-plane directions [7]. In thick FeGa thin films, the residual strain can introduce the well-known stripe phase structure [8] due to the presence of weak ME perpendicular anisotropy contribution to the anisotropy energy.

The Fe_{100-x}Ga_x/MgO system can incorporate to the rich oxide-3d metal interface physics [9] strong magnetoelastic (ME) coupling of the FeGa alloy. The overlap between orbitals of *O* and *Fe* metal induces large values for the interface anisotropy constant K_s [10], and the ME

contribution could be also used to manipulate the magnetic anisotropy if the film is grown onto a ferroelectric layer [11], besides of the modification of the electronic structure by the application of electric field [12]. The study of the magnetic domain configuration in thin films is a tool to insight about the presence of competing interactions demonstrating the role of volume, as for instance the ME energy due to the coupling between magnetic moment and strain [13], as well as interface contributions [14] to the total magnetic anisotropy, in domain structures not observed in bulk materials. In polycrystalline films, the magnetization can be not homogeneous, generating the effect known as magnetization ripple [15]. The explanation of the fluctuations of \mathbf{M} is based on the irregular magnetocrystalline anisotropy of the randomly distributed crystallites. The model description incorporates the statistical treatment of local randomly oriented anisotropy and a uniform magnetic anisotropy [16].

Here we present a study of the magnetic domain structure of Fe_{100-x}Ga_x films grown on MgO(001) as function of x performed by magnetic force microscopy (MFM). We show that the presence of a domain structure in Fe_{100-x}Ga_x films evolves from an in-plane disposition of the magnetization to a corrugated domain structure, with periodicities in the range of hundreds of nanometers, as the Ga content increases. Because of the weakness of both volume and interface perpendicular anisotropies, the role of the disorder introduced by the formation of secondary phases as the Ga content increases is discussed. Therefore, the presence of a corrugation of the domain images is related to the presence of a weak random magnetic anisotropy superimposed to the coherent cubic regular contribution.

x (% Ga)	t_f (nm)	$K_{(100)}$ (nm^{-1})	$\Delta K_{(100)}$ (nm^{-1})	$K_{(200)}$ (nm^{-1})	$\Delta K_{(200)}$ (nm^{-1})	L (nm)	ϵ
13	17	-	-	6.967	0.156	-	-
21	16	3.438	0.143	6.925	0.185	7.1	0.010
24	20	3.468	0.107	6.930	0.172	12.1	0.011
28	21	3.451	0.081	6.912	0.132	16.6	0.009
28	56	3.406	0.099	6.848	0.146	11.7	0.010

TABLE I. Composition and thickness used to identify the samples grown at $T_s = 150$ °C presented in this study. Reciprocal space position and Full Width at Half Height (ΔK) for (001) and (002) reflections obtained with Gaussian curve fit. K is defined as $2\sin\theta/\lambda$ and ΔK is $\cos\theta\Delta(2\theta)/\lambda$. L and ϵ are obtained performing the fit of the (001) and (002) reflections with the Williamson-Hall model.

EXPERIMENTAL RESULTS

Thin film preparation

The samples studied here have been grown by Molecular Beam Epitaxy in a process described elsewhere [17], with the substrate temperature T_s set at 150 °C. The films are grown directly on the MgO(001) surface after as-received substrates are heated at 800 °C for four hours, in UHV conditions. RHEED pictures show Kikuchi patterns indicating the cleanness of the surface. The film thickness t_f ranges between 20 nm to 56 nm and all of them were covered with a block of Mo. Magnetic properties were investigated by vibrating sample magnetometry (VSM) and magnetic force microscopy (MFM) in air and low vacuum. A Rigaku rotating anode D/max 2500 diffractometer working with a Bragg-Brentano configuration with the $K_{\alpha,Cu}$ wavelength was used to perform *ex situ* structural characterization. For the film with $x=28$ and $t_f=56$ nm, the beamline BM25A at the European Synchrotron Radiation Facility (ESRF), Grenoble, France with $\lambda = 0.062$ nm was used. Dispersive X-ray spectroscopy (EDX) and X-ray reflectivity were used to determine composition and film thickness. Table I presents the relevant structural data of the films used in this study. The samples are referred in the text with two of numbers describing composition and thickness, thus 13-17 stands for the film with Ga content 13 % and $t_f = 17$ nm.

Magnetic force microscopy images

Figure 1 shows atomic force microscopy images on films grown at $T_s = 150$ °C and $T_s = 600$ °C with *bcc* crystal structure [17]. The image of the films grown at $T_s = 150$ °C, obtained from sample 24-20, is representative of the topography of the films studied by MFM. By elevating T_s , the roughness increases and the film surface looks like a set of domes, notice that the gray scale is larger and the

window length side smaller for the films with $T_s = 600$ °C than for the films with $T_s = 150$ °C. Similar transition from 2- to 3- dimensional growing has been reported for pure Fe films grown on MgO [18]. The image taken for the films grown at 150 °C shows also some steps due to the MgO [110] edges, the height of which is about 0.4 nm (measured for the steps crossing the black line in Fig 1a).

Magnetic force microscopy images presented in Fig 2 were performed in air (a)-(d) and in low vacuum (e)-(f) for the films listed in table I. Film 13-17 (see Fig 2a) shows lines on the film surface separating areas without contrast and also some tip induced features; the image displayed in Fig 2b, taken for film 24-20, shows a fine structure which is not observed in the areas separating the domains walls of the image 2a for film 13-17. Fig 2c and 2d shows the same kind of magnetic contrast, revealing a non uniform magnetic configuration, in more detail for films with 28-56 and 28-21, respectively. For sample 21-16 strength of the corrugation is very weak for in-air measurements (not shown). These features do not change after performing several scans on the same area of the sample.

The sensitivity of the measurement is enlarged by performing the measurements in low vacuum. Thus for film 13-17 the image displays only the contrast due to the domain walls (see Fig 2e) without the trace of any other sub-structure, while for sample 21-16 the corrugation becomes very clear (see Fig 2f). A rough comparison of the strength of the contrast for both kind of domain structures is performed considering the range of the variation of the signal for films 13-17 (see Fig 2e) and 21-16, because these measurements were obtained in similar in-vacuum conditions. The magnetic signal of sample 21-16 is in the range of ± 1.5 units, small compared with that due to the domain walls of film 13-17, which is ± 7 units. The inset of Fig 2f represents an image of the film 21-16 in the range of ± 7 units. For the films with $x > 21$ the corrugation is clearly observed in the air images, although the sensitivity is smaller for this measurements (see that the larger scale is now limited to ± 0.5 units) because of the increment of the width resonance of the tip in air with respect to vacuum. The period of these ripple structures is about 300 nm for samples 24-20, 28-56 and 28-21 and 900 nm for film 21-16.

The lines in image Fig 2a and e can be interpreted as domain walls separating areas with in-plane magnetization and are the expected result for thin films without significant out-of-plane contributions. The texture of the images changes for the films with $x > 20$, for which areas with alternating contrast are observed, see fig 2c-d. This domain structure is obtained in remnant state achieved after applying field along the in-plane direction. Features in MFM images in bulk samples are explained by a sample preparation process that can induce stresses and other defects[19]. However, the thin films presented here have not been treated after growth and the observed fea-

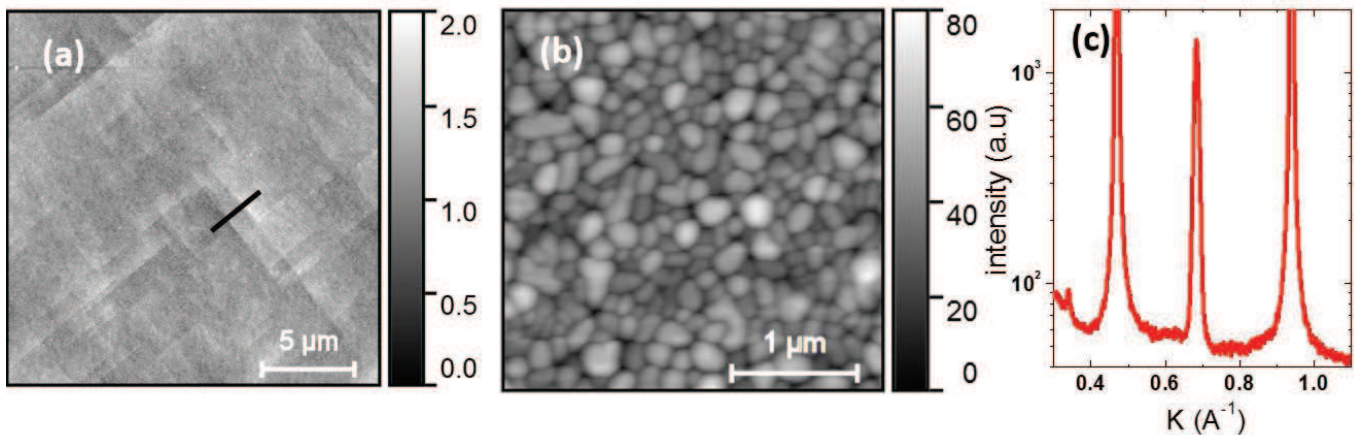


FIG. 1. Topographic images taken on films grown at (a) $T_s = 150$ °C (sample 24-20) and (b) $T_s = 600$ °C. The color bar key units are nm. The height of the steps along the thick line in panel *a* are about 0.4 nm. (c) X-ray diffraction data, with $K(=2\sin\theta/\lambda)$ perpendicular to the film plane, for sample 28-56.

tures cannot be attributed to any post-growing processing. In bulk samples, large domains have been observed without fine magnetic structures in quenched in water or slowly cooled single-crystals [19–21]. These domains resemble the domains obtained for films with low Ga contents seen in Figure 2a, because the magnetic contrast is only due to the presence of domain walls. The magnetic contrast corrugation in thin films has been explained due to the presence of a magnetic anisotropy that competes with the magnetostatic term. Thus, volume perpendicular magnetic anisotropy (Ni [13] and FeGa[8] films), interface magnetic anisotropy (in Co/Pt multilayers with canted magnetization [14]) and random magnetic anisotropy in polycrystalline films [15] generate the stripe and ripple domain configurations.

Magnetization loops

A consequence of non-homogeneous domain structure concerns the magnetization curves: if \mathbf{M} has some degree of out-of-plane component, the remanent magnetization M_r has to be lower than the saturation value M_s [8, 13, 14]. Figure 3(a) shows M vs $\mu_0 H$ for a maximum applied field of 9 T along the in-plane easy direction. This measurement allows subtracting linear diamagnetic contributions with the slope obtained at large field ($\mu_0 B > 6$ T). A correction performed in loops that reach lower values of the maximum field can yield a M_r equal to M_s , see the loop performed up to 0.15 T in Figure 3(a)inset. For the loop taken for sample 28-56, it can be noted that M_r is large, around $0.95M_s$ but a field of about 1.6 T is needed to reach the full saturation.

The magnetic hysteresis loops performed for sample 28-56, with the applied field along the [100] and [110] directions, see Fig 3 (inset) show that the in-plane [110]

axis is the magnetization easy direction. These measurements indicate a spin reorientation of \mathbf{M} with respect to reference Fe/MgO(100) films where the easy direction is the $\langle 100 \rangle$ axis, a behaviour observed in bulk crystals [22] and other epitaxial thin films under tensile [7] or compressive [23] stress. For the (001) plane the magneto-crystalline energy density $e_{mc}(\phi)$ can be expressed as $K_1 \sin^2 \phi \cos^2 \phi$, with K_1 the magnetic anisotropy constant and ϕ the angle that forms \mathbf{M} and the [100] direction. K_1 can be estimated evaluating the energy required to saturate the film along each direction. The measurement for films with $x = 28$ gives rise to a value of about -10 kJ/m³ for K_1 .

The need of large magnetic field to reach a full saturation cannot be explained by mis-orientation between sample and magnetic field since the magnitude of the anisotropy constant is small, around 10 kJ/m³. Therefore, the lack of magnetization at low field can be associated with the presence of the domain structure observed in MFM images.

X-ray diffraction

The films presented here have been studied previously by X-ray diffraction [17]. For film 28-56, a scan has been done by means of synchrotron radiation light with $\lambda = 0.062$ nm, see Figure 1c and $K(=2\sin\theta/\lambda)$, perpendicular to the film plane. The out-of-plane and in-plane lattice parameter value decreases and increases, respectively, with respect to the bulk value because of the effect of the epitaxial strain due to the MgO substrate [17]. Regarding the ordering of the Ga and Fe atoms, a superlattice (001) peak is observed for x above 20, together with the (002) peak due to the *bcc* structure. The width $\Delta K_{(00n)}$ of those peaks fitted using a gaus-

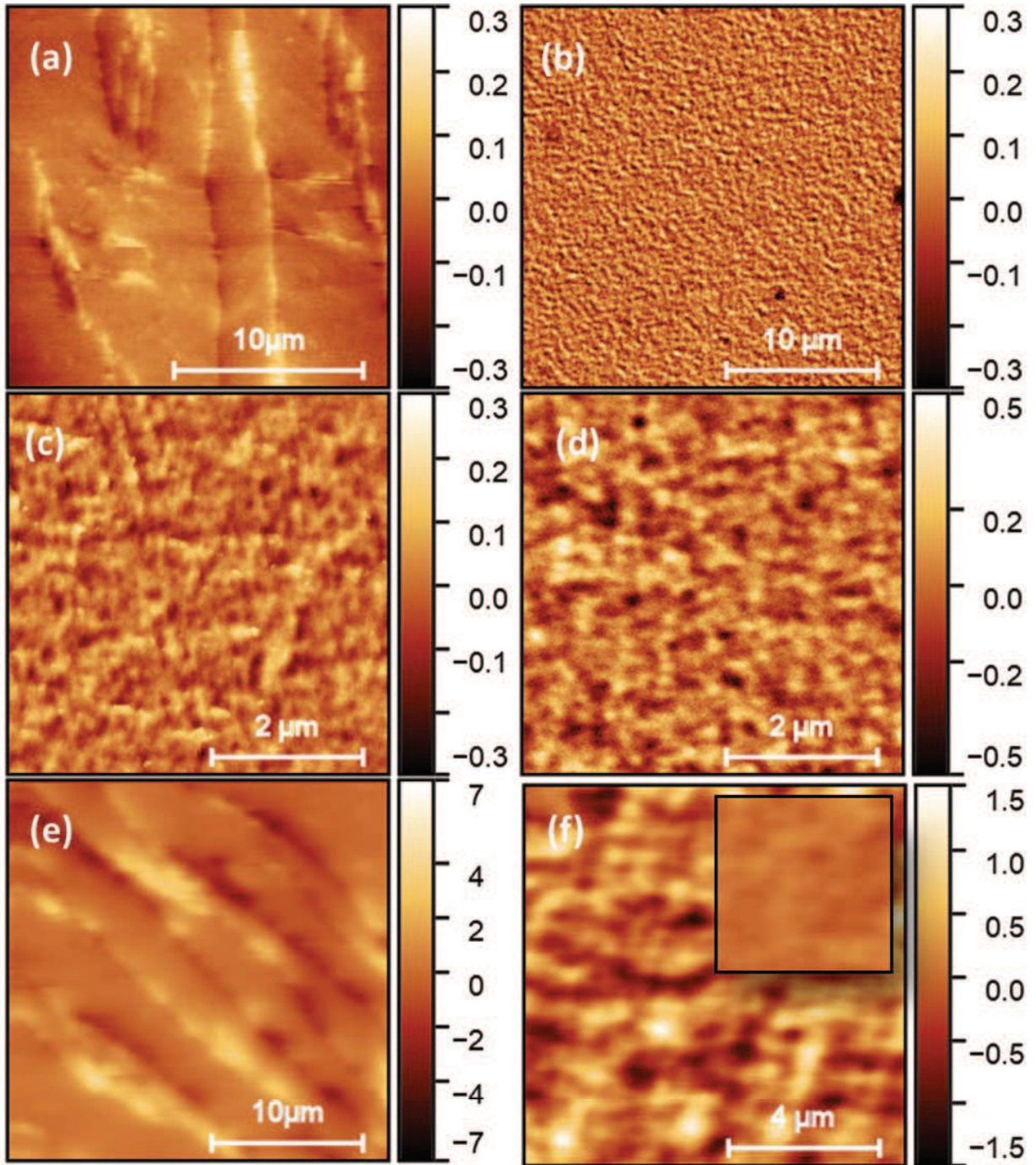


FIG. 2. Magnetic force microscopy images taken in air for films (a) 13-17 (b) 24-20 (c) 28-56 nm (d) 28-21, and in low vacuum for films (e) 13-17 and (f) 21-16, the color scale for the inset is ± 7 .

sian functions is presented in Table I. The effect on ΔK due to $K_{\alpha,1}$ and $K_{\alpha,2}$ peaks can be quantified by considering the splitting of the MgO substrate (002) and (004) reflections as well as other instrumentation effect, being the corrections to the values obtained with the Gaussian fit negligible. The increment of $\Delta K_{(002)}$ with respect to $\Delta K_{(001)}$ suggests the presence of inhomogeneous strain produced by factors such as dislocations, non-uniform

distortions, or antiphase domain boundaries and it has been addressed as the reason to observe enlargement of ΔK with K [24]. The Williamson-Hall method applied to gaussian fits [24, 25] relates $\Delta K_{(00n)}$ with the average crystallite size L and strain ϵ in the film by the equation $\Delta K_{(n00)}^2 = (0.9/L)^2 + 4\epsilon^2 K^2$. The values obtained can be seen in table I. Notice that the value obtained for L is not limited by the film thickness and ϵ values are in the

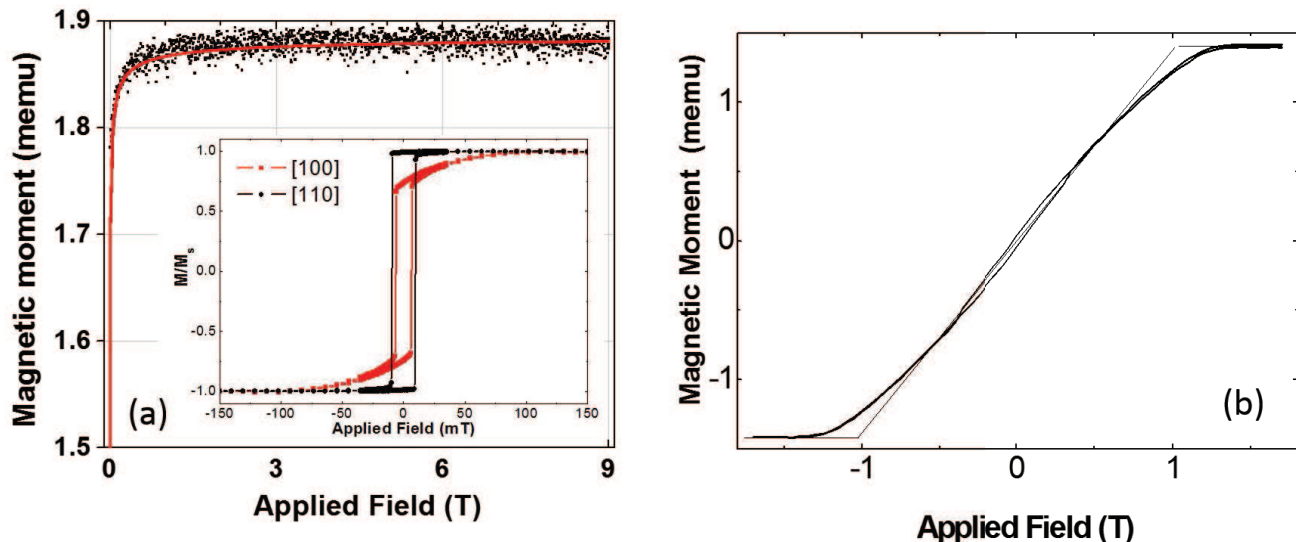


FIG. 3. (a) Detail of the magnetization loop with applied field up to 9 T along the easy direction for sample 28-56, red line is a fit described in the text. Inset. MB loops in the low field range (± 150 mT) for [110] and [100] in-plane directions. (b) M-H loop along the axial [001] direction for sample 28-21. The line is a fit used to calculate the slope at zero field and evaluate the effective magnetic anisotropy constant.

range of 10^{-2} .

This result indicates that the film strain is inhomogeneous. The misfit between FeGa and MgO decreases since the bulk lattice parameter of the FeGa alloy increases with Ga content and gets closer to $\sqrt{2}a_{MgO} \approx 2.977$, a fact that discards the nucleation of misfit dislocations as the origin for an increment of the value of ϵ , and suggests effects that appear with the increment of Ga content.

We propose that crystal structures with crystal regions with ordered and random distribution of Ga/Fe species, corresponding to slightly different lattice parameters [26] coexist in the films and contribute to enlarge the inhomogeneous strain in the film. Therefore the effect of a better matching with the MgO substrate is diminished.

ANALYSIS

Here, we analyze several contribution to the magnetic energy that can play a role in order to explain the observation of inhomogeneous domain structures.

Perpendicular magnetic anisotropies

The microscopic modulation on the magnetization vector has been ascribed to the competition of the perpendicular and shape anisotropies. Several models predict, in terms of volume or interface perpendicular contribution strength, the range of thicknesses that hold a configuration for \mathbf{M} with an out-of-plane component.

Volume anisotropies

The standard model establishes the presence of stripe phase in terms of the parameter $K_u/(0.5\mu_0M_s^2) = Q$ with K_u being a perpendicular magnetic anisotropy constant. For $Q < 1$, the film thickness has to be larger than the critical value to develop a stripe structure [27]. Figure 3b shows a representative M-H loop, with H perpendicular to the film, for sample 28-21. The thin line corresponds to the linear fit of $M(H)$ used to evaluate the perpendicular anisotropy constant through the anisotropy field H_a , and provides $\mu_0H_a \approx 1$ T for the intersection with $M = M_s$. In the case of a sole magnetostatic contribution to K_u , $\mu_0H_a = \mu_0M_a$. However, several values for μ_0M_s are reported in the literature for compositions around $x = 28$, ranging from ≈ 1.4 T [28] to around 1.15 T [26, 29]. Our VSM measurements provide for the film 28-56, see Fig 3, a value for μ_0M_s of about 1.2 T.

For the films presented, the ME contribution does not induce perpendicular anisotropy because the signs of the film strains [17] and the B_1 ME coefficient result in a contribution that favors the in-plane orientation of \mathbf{M} . The contribution due to an asymmetric distribution of the NNN Ga-Ga pairs proposed to explain the anisotropies in other Fe-Ga films could also explain the presence of a positive K_u [8]. The simplest estimation of K_u can be done by assuming that the total in-plane anisotropies correspond to $0.5\mu_0M_s^2$. Considering $\mu_0M_s = 1.2$ T and with the value of $\mu_0H_a \approx 1.0$ T, $Q \approx 0.17$. However, the stripe model for $Q = 0.17$ and $A = 15$ pJ/m predicts in-plane magnetization for films thickness below 71 nm, a value larger than that for the films studied here, with

values below 60 nm. Decreasing Q will increase the range of film thickness with in-plane magnetization. The same calculation for $Q = 0.15$, that can be obtained by adding the in-plane ME anisotropy increases the critical thickness up to 78 nm. Therefore, a simple estimation for the volume perpendicular anisotropy, if it were present in the films, does not explain the domain structure observed as the gallium content increases.

Surface anisotropy on the Fe-MgO interface and canting

Several works indicate that K_s due to Fe/non-metallic interfaces can be large since perpendicular magnetic orientation has been observed in thin Fe layers sandwiched by MgO blocks [30] and canting of M in Fe/MgO films [31]. K_s can be as large as 2 mJ/m² and first principles calculations give values of about 3 mJ/m² for ideal MgO/Fe interface [10].

Micromagnetic models [32, 33] analyze the canting of the magnetization due to a surface/interface contribution assuming that the tilting angle can change only along the axial direction and is uniform on each film plane. Both models do not consider the presence of a domain structure, but the results of this analysis provides a starting point to analyze the effect of K_s . Thus, the magnetization state can be in a canted phase, in certain range of film thicknesses, between perpendicular and in-plane magnetization state [33]. In order to find the critical thickness for which FeGa/MgO is in the canted state we use $\mu_0 M_s = 1.1$ T and $A = 15$ pJ/m. Phase diagram in [33] is presented for symmetric structures but expressions for asymmetrical interface anisotropies are also obtained. For the Fe/Mo interface K_s is probably positive and large because a value of about 2 mJ/m² is reported for Mo/CoFeB layers [34]. Therefore, a first analysis is done with the same value of K_s for both interfaces, having in mind that lower values of K_s reinforce in-plane magnetization. For $K_s = 1.5$ mJ/m², the model yields a canted state for films with thickness between 5.6 and 6.9 nm, values well below the film thickness. Therefore, although K_s can be large, it is insufficient to deviate \mathbf{M} from lying on the film plane.

Random and coherent magnetic anisotropy: Thin film vs bulk

Several models, calculations and experiments deal with the effects that the presence of a random magnetic anisotropy (RMA), added to the coherent magnetic anisotropy term, has on the magnetic behavior of crystalline materials. A ferromagnetic with wandering axis (FWA) phase, a magnetic state with the magnetization twisting around the magnetic easy axis, is proposed as the result of the competition between coherent and weak

random contributions. Therefore the magnetic order is ferromagnetic but the random anisotropies induce local axis than produce a deviation of the magnetization vector inside the ferromagnetic domain [35]. A system with weak random anisotropy, generated by dilution of a non-magnetic ion, and cubic anisotropy shows in its phase diagram the presence of ferromagnetic phase with low remanence between the ferromagnetic and the spin glass phases as the non-magnetic ion concentration increases [36]. Montecarlo simulations predict a domain ferromagnetic phase, in between of the ordinary ferromagnetic and spin-glass phases in a cubic spin model with random anisotropic exchange [37].

A consequence of the presence of RMA in magnets with a coherent anisotropy is that the saturation magnetization approach law in a FWA state is given by the expression [35]:

$$\frac{M(H) - M_s}{M_s} = \frac{1}{15} \frac{H_r^2}{[H_{ex}^3 (H + H_c)]^{1/2}} \quad (1)$$

where H_{ex} , H_r and H_c correspond to the exchange, random and coherent anisotropy fields defined in ref [35]. Considering $\mu_0 H_c M_s = (1/4)K_1$, we obtain $H_c = 2 \times 10^3$ A/m for $M_s = 10^6$ A/m and $|K_1| = 10$ kJ/m³. The high field magnetization curve measured in film 28-56 is simulated (see red curve Fig 2) with $H_c \approx 2 \times 10^3$ A/m and $H_r^2/H_{ex}^{3/2} = 1.5 \times 10^4 \sqrt{A/m}$. Therefore, the presence of FWA state can explain the experimental magnetization process.

Another output of this model is that the magnetic correlation length is given by $\delta_m = [A_r/K]^{1/2}$ [35]. With values for $A_r = 15$ pJ/m and $K = K_1$, $\delta_m \approx 40$ nm. This value is clearly smaller than the corrugation observed by MFM. However the MFM images show the whole landscape of the magnetic state, therefore the transitions between regions with different orientation of M cannot be performed by sharp domain walls because the exchange energetic cost and, at least, would require several units of segments with length δ_m . Thus, the oscillation of the magnetic signal is the result of the twist of M in several steps, each one with a length of about δ_m . We note that the periodicity of the domain structure in RMA films with values larger than δ_m has been observed previously in TbFe₂ amorphous films [38].

The effect of the disorder due to defects depends on the strength of the local magnetic anisotropy compared with other microscopic parameters. Usually local disorder is small and unable to break the long range correlation length, thus microscopic images show homogeneous areas separated by domain walls, although polycrystalline films can show a ripple of the \mathbf{M} [15]. Defects existing in FeGa samples with low Ga content and different preparation procedures show uniform magnetization in the single domain areas separated by domain walls. The defects manifest themselves by domain wall pinning and by modifying the coercive field.

Here, the differences between bulk samples and thin films are presented to explain the presence of random anisotropies in the films that justify the breaking of a uniform orientation of \mathbf{M} in each magnetic domain. The variation of NNN Ga-Ga distribution in the film, the microstrain in grains and the interface magnetic anisotropy are discussed. All the above factors increase the RMA contributions to the energy with the Ga content.

Ga-Ga pairing mechanism

NNN Ga-Ga pairs are able to generate a local strain and therefore a large magnetic anisotropy. The model to explain the variation of the cubic coherent anisotropy [6] suggests that the anisotropy constant of each pair can be large, $\sim 10^7$ J/m³, but spatial averaging results in an effective fourfold anisotropy about 2-3 orders of magnitude smaller. In thin films, an anisotropic distribution of Ga-Ga pairs between the in-plane and the out-of plane direction is proposed to produce a contribution to the perpendicular anisotropy as large as $\sim 10^5$ J/m³ [7]. However, the distribution of the Ga-Ga pairs can be inhomogeneous due to the nucleation of ordered FeGa phases and alter locally the average performed in refs [6, 7] to obtain the effective values of the anisotropy coefficients.

Let's assume that the local anisotropy is generated by the Ga-Ga pairs. In an A2 matrix the distribution of Ga-Ga pairs is homogeneous on the whole volume of the film, independently of the grain size, and each grain has a similar contribution to the anisotropy energy as happens in a single element film. Increasing the Ga content introduces a metastable state with a ordered secondary phase and the distribution of those Ga-Ga pairs becomes inhomogeneous since it is random in the volume of the A2 phase and fixed in the inclusions. That number of pairs is null considering D0₃ structure, but above the average of the A2 phase if the B2 structures is considered.

Grain size and micro-strain

Another feature observed in the thin film concerns the comparison of ΔK obtained in this study with bulk samples [39]. $\Delta K_{(002)}$ in the films is at least one order of magnitude smaller for bulk samples while $\Delta K_{(001)}$ takes values of the same order of magnitude for both kind of samples. In bulk material the volume of the secondary phase is small compared with the main phase and can behave as pinning centers for domain walls. However, in thin films the analysis of the peak widths suggests that the volume of the grains of the phases is small and with comparable values. On the other hand, the significant deviation of the strain in the film suggests a way to alter the anisotropy locally, through the ME effect in each grain on the film.

Interface magnetic anisotropy

Last but not least, at the film interface with MgO, the local fluctuations of the Fe/Ga atoms distribution can introduce another source of randomness since the interface contribution per atom is expected to disappear for the Ga-O bond. The ordered phases are formed by two kind of layers, Fe atoms and an ordered mix of Fe and Ga atoms. Thus, the larger value of K_s will be expected for grains that has a layer without Ga atoms at the interface, as happens for one half of the layers of the D0₃ and B2 structures; in areas with layers with gallium, K_s will be halved for the D0₃ phase or nulled for the B2 one. For the disordered phase the interface contribution will be proportional to the Fe composition and K_s will go with $100-x/100$.

CONCLUSIONS

In epitaxial thin films of FeGa grown on MgO(001) substrates the magnetic domain structure evolves from a uniform in-plane magnetization to a state with non-collinear configuration as the Ga content increases. The crystalline phase distribution can generate local inhomogeneous distributions of Fe/Ga atoms through the film volume and on the interface with the MgO substrate as well as local strains. As a result, a random magnetic anisotropy able to break the uniform magnetization in the magnetic domains due to the coherent cubic magnetic term is proposed to explain the observed domain structures.

ACKNOWLEDGMENTS

This work has been supported by Spanish MICINN (Grant No. MAT2015-66726-R) and Gobierno de Aragón (Grant E10-17D) and Fondo Social Europeo. Authors would like to acknowledge the use of Servicio General de Apoyo a la Investigación-SAI, Universidad de Zaragoza as well as Surface and Coating Characterization Service at CEQMA (CSIC-Universidad de Zaragoza). We acknowledge the use of the microscopy infrastructure available in the Laboratorio de Microscopías Avanzadas (LMA) at Instituto de Nanociencia de Aragón (University of Zaragoza, Spain). AB thanks MINECO for the Ph. D. grant BES-2016-076482.

* miguel.ciria@csic.es

[1] Arthur E. Clark, James B. Restorff, Marilyn Wun-Fogle, Thomas A. Lograsso, and Deborah L. Schlager. Magnetostrictive properties of body-centered cubic Fe-Ga and

- Fe-Ga-Al alloys. *IEEE Trans. Magn.*, 36(5 1):3238–3240, 2000.
- [2] A. E. Clark, M. Wun-Fogle, J.B. Restorff, T.A. Lograsso, and J.R. Cullen. Effect of quenching on the magnetostriction on $\text{Fe}_{1-x}\text{Ga}_x$ ($0.13 < x < 0.21$). *IEEE Trans. Magn.*, 37(4):2678–2680, 2001.
- [3] A. E. Clark, K. B. Hathaway, M. Wun-Fogle, J. B. Restorff, T. A. Lograsso, V. M. Keppens, G. Petculescu, and R. A. Taylor. Extraordinary magnetoelasticity and lattice softening in bcc Fe-Ga alloys. *J. Appl. Phys.*, 93(10 3):8621–8623, 2003.
- [4] He Yangkun, Ke Xiaoqin, Jiang Chengbao, Miao Naihua, Wang Hui, Coey John Michael David, Wang Yunzhi, and Xu Huibin. Interaction of Trace Rare-Earth Dopants and Nanoheterogeneities Induces Giant Magnetostriction in Fe-Ga Alloys. *Adv. Funct. Mater.*, 28(20):1800858, 2018.
- [5] O Ikeda, R Kainuma, I Ohnuma, K Fukamichi, and K Ishida. Phase equilibria and stability of ordered b.c.c. phases in the Fe-rich portion of the FeGa system. *J. Alloys Compd.*, 347(1):198 – 205, 2002.
- [6] J. Cullen, P. Zhao, and M. Wuttig. Anisotropy of crystalline ferromagnets with defects. *J. Appl. Phys.*, 101(12), 2007.
- [7] M. Barturen, J. Milano, M. Vázquez-Mansilla, C. Helman, M. A. Barral, A. M. Llois, M. Eddrief, and M. Marangolo. Large perpendicular magnetic anisotropy in magnetostrictive $\text{Fe}_{1-x}\text{Ga}_x$ thin films. *Phys. Rev. B*, 92:054418, Aug 2015.
- [8] S. Tacchi, S. Fin, G. Carlotti, G. Gubbiotti, M. Madami, M. Barturen, M. Marangolo, M. Eddrief, D. Bisero, A. Rettori, and M. G. Pini. Rotatable magnetic anisotropy in a $\text{Fe}_{0.8}\text{Ga}_{0.2}$ thin film with stripe domains: Dynamics versus statics. *Phys. Rev. B*, 89:024411, Jan 2014.
- [9] B. Dieny and M. Chshiev. Perpendicular magnetic anisotropy at transition metal/oxide interfaces and applications. *Rev. Mod. Phys.*, 89:025008, Jun 2017.
- [10] H. X. Yang, M. Chshiev, B. Dieny, J. H. Lee, A. Manchon, and K. H. Shin. First-principles investigation of the very large perpendicular magnetic anisotropy at Fe|MgO and Co|MgO interfaces. *Phys. Rev. B*, 84:054401, Aug 2011.
- [11] Sasikanth Manipatruni, Dmitri E. Nikonov, Chia-Ching Lin, Tanay A. Gosavi, Huichu Liu, Bhagwati Prasad, Yen-Lin Huang, Everton Bonturim, Ramamoorthy Ramesh, and Ian A. Young. Scalable energy-efficient magnetoelectric spin-orbit logic. *Nature*, December 2018.
- [12] T. Maruyama, Y. Shiota, T. Nozaki, K. Ohta, N. Toda, M. Mizuguchi, A. A. Tulapurkar, T. Shinjo, M. Shiraishi, S. Mizukami, Y. Ando, and Y. Suzuki. Large voltage-induced magnetic anisotropy change in a few atomic layers of iron. *Nat. Nanotechnol.*, 4:158, January 2009.
- [13] M. A. Marioni, N. Pilet, T. V. Ashworth, R. C. O’Handley, and H. J. Hug. Remanence due to Wall Magnetization and Counterintuitive Magnetometry Data in 200-nm Films of Ni. *Phys. Rev. Lett.*, 97:027201, Jul 2006.
- [14] Robert Frömter, Holger Stillrich, Christian Menk, and Hans Peter Oepen. Imaging the cone state of the spin reorientation transition. *Phys. Rev. Lett.*, 100:207202, May 2008.
- [15] Harrison W. Fuller and Murray E. Hale. Determination of magnetization distribution in thin films using electron microscopy. *J. Appl. Phys.*, 31(2):238–248, 1960.
- [16] K. J. Harte. Theory of largeangle ripple in magnetic films. *Journal of Applied Physics*, 37(3):1295–1296, 1966.
- [17] M Ciria, M G Proietti, E C Corredor, D Coffey, A Begué, C de la Fuente, J I Arnaudas, and A Ibarra. Crystal structure and local ordering in epitaxial $\text{Fe}_{100-x}\text{Ga}_x/\text{MgO}(001)$ films. *J. Alloys Compd.*, 767:905–914, 2018.
- [18] C Boubeta-Martínez, J L Costa-Krämer, and A Cebollada. Epitaxy, magnetic and tunnel properties of transition metal/MgO(001) heterostructures. *J Phys: Condens Matter*, 15(25):R1123–R1167, 2003.
- [19] Chaitanya Mudivarthi, Suok M. Na, Rudolf Schaefer, Mark Laver, Manfred Wuttig, and Alison B. Flatau. Magnetic domain observations in Fe-Ga alloys. *J. Magn. Mater.*, 322(14):2023–2026, 2010.
- [20] Q. Xing and T. A. Lograsso. Magnetic domains in magnetostrictive FeGa alloys. *Appl. Phys. Lett.*, 93(18):182501, 2008.
- [21] Yangkun He, J. M. D. Coey, Rudolf Schaefer, and Chengbao Jiang. Determination of bulk domain structure and magnetization processes in bcc ferromagnetic alloys: Analysis of magnetostriction in $\text{Fe}_{83}\text{Ga}_{17}$. *Phys. Rev. Materials*, 2:014412, Jan 2018.
- [22] Sadia Rafique, James R. Cullen, Manfred Wuttig, and Jun Cui. Magnetic anisotropy of FeGa alloys. *J. Appl. Phys.*, 95(11 II):6939–6941, 2004.
- [23] Adam McClure, S. Albert, T. Jaeger, H. Li, P. Rugheimer, J. A. Schaefer, and Y. U. Idzerda. Properties of single crystal $\text{Fe}_{1-x}\text{Ga}_x$ thin films. *J. Appl. Phys.*, 105(7):07A938, 2009.
- [24] G.K Williamson and W.H Hall. X-ray line broadening from filed aluminium and wolfram. *Acta Metall.*, 1(1):22 – 31, 1953.
- [25] T. D. Shen, R. B. Schwarz, and J. D. Thompson. Soft magnetism in mechanically alloyed nanocrystalline materials. *Phys. Rev. B*, 72:014431, Jul 2005.
- [26] Nobuo Kawamiya, Kengo Adachi, and Yoji Nakamura. Magnetic Properties and Mossbauer Investigations of Fe-Ga Alloys. *J. Phys. Soc. Jpn.*, 33(5):1318–1327, 1972.
- [27] Alex Hubert and Rudolf Schfer. *Magnetic Domains*. Springer-Verlag Berlin Heidelberg, 1998.
- [28] C. Bormio-Nunes, M. a. Tirelli, R. Sato Turtelli, R. Grössinger, H. Muöller, G. Wiesinger, H. Sassik, and M. Reissner. Volume magnetostriction and structure of copper mold-cast polycrystalline Fe-Ga alloys. *J. Appl. Phys.*, 97(3):033901, 2005.
- [29] Jayasimha Atulasimha, Alison B Flatau, and James R Cullen. Analysis of the effect of gallium content on the magnetomechanical behaviour of single-crystal FeGa alloys using an energy-based method. *Smart Mater. Struct.*, 17:025027, 2008.
- [30] J. Balogh, I. Dézsi, Cs. Fetzter, J. Korecki, A. Koziol-Rachwał, E. Młyńczak, and A. Nakanishi. Magnetic properties of the Fe-MgO interface studied by Mössbauer spectroscopy. *Phys. Rev. B*, 87:174415, May 2013.
- [31] Taizo Kawauchi, Yoshio Miura, Xiaowei Zhang, and Katsuyuki Fukutani. Interface-driven noncollinear magnetic structure and phase transition of Fe thin films. *Phys. Rev. B*, 95:014432, Jan 2017.
- [32] R. C. O’Handley and J. P. Woods. Static magnetization direction under perpendicular surface anisotropy. *Phys. Rev. B*, 42:6568–6573, Oct 1990.
- [33] A. Thiaville and A. Fert. Twisted spin configuration in thin magnetic layers with interface anisotropy. *J. Magn.*

- Magn. Mater.*, 113:161, 1992.
- [34] T. Liu, Y. Zhang, J. W. Cai, and H. Y. Pan. Thermally robust Mo/CoFeB/MgO trilayers with strong perpendicular magnetic anisotropy. *Sci. Rep.*, 4:5895, July 2014.
- [35] E. M. Chudnovsky, W. M. Saslow, and R. A. Serota. Ordering in ferromagnets with random anisotropy. *Phys. Rev. B*, 33:251–261, Jan 1986.
- [36] A. del Moral, J. I. Arnaudas, P. M. Gehring, M. B. Salamon, C. Ritter, E. Joven, and J. Cullen. Magnetic first-order phase transition and crossover associated with random anisotropy in crystalline $\text{Dy}_x\text{Y}_{1-x}\text{Al}_2$. *Phys. Rev. B*, 47:7892–7896, Apr 1993.
- [37] Ronald Fisch. Phase transitions in cubic models with random anisotropic exchange. *Phys. Rev. B*, 51:6358–6363, Mar 1995.
- [38] F. Hellman, A. L. Shapiro, E. N. Abarra, R. A. Robinson, R. P. Hjelm, P. A. Seeger, J. J. Rhyne, and J. I. Suzuki. Long ferromagnetic correlation length in amorphous TbFe_2 . *Phys. Rev. B*, 59:11408–11417, May 1999.
- [39] Y. Du, M. Huang, T. a. Lograsso, and R. J. McQueeney. X-ray diffuse scattering measurements of chemical short-range order and lattice strains in a highly magnetostrictive $\text{Fe}_{0.813}\text{Ga}_{0.187}$ alloy in an applied magnetic field. *Phys. Rev. B*, 85(21):1–6, 2012.